World Journal of Engineering Research and Technology
WJERT
www.wjert.org
SJIF Impact Factor: 4.326

APPLICATION OF NUMERICAL OPTIMIZATION AS A TOOL FOR VALIDATION OF OPTIMIZED RESPONSE OF FLEXURAL STRENGTH OF WOOD ASH (HARDWOOD) PARTICLES REINFORCED POLYPROPYLENE WARPP

Aguh Patrick Sunday*[1] and Ejikeme Ifeanyi Romanus[2]

[1]Department of Industrial Production Engineering, Nnamdi Azikiwe University, Awka, Anambra State, Nigeria.

[2]Office of the Commissioner, Ministry of Environment, Beautification and Ecology, Awka, Anambra State, Nigeria.

Article Received on 22/06/2017 **Article Revised on 12/07/2017** **Article Accepted on 02/08/2017**

***Corresponding Author**
Aguh Patrick Sunday
Department of Industrial Production Engineering, Nnamdi Azikiwe University, Awka, Anambra State, Nigeria.

ABSTRACT

In this study, we investigated the adequacy of approximation of fitted model to the real system. To meet this objective, the numerical optimization method was applied as an alternative to the conventional method by Suresh (2014) for the validation of optimized performance characteristic (response) model. Box – Behnken design, a spherical design, with all factorial and axial points at the same distance from the center of the design was used to build a model for predicting and optimizing the flexural strength of WARPP. The mathematical model equations (response surface models) were derived from the response surface methodology (RSM) optimization process using Minitab 16 software. This response surface model is representable with nonlinear power equation and second order polynomial of the four control factors. In the statistical analysis, the analysis of variance (ANOVA) table, the coefficient of determination, R^2 and the adjusted coefficient of determination, R^2_{adj} values and p values indicated that the model was adequate for representing the experimental data. The p values show that the linear effects of volume fraction (B), injection force (C), operating temperature (D) and quadratic effects of volume fraction (B^2), injection force (C^2) and the interaction effects of volume fraction and

injection force (B*C) and volume fraction and operating temperature (B*D) were highly significant. To gain a better understanding of the control variables for optimal flexural performance, the graphical models were presented as 3 – D response surface and 2 – D contour graphs. The optimal setting for the particle size (A), volume fraction (B), injection force (C) and operating temperature (D) were found to be 1.40mm, 5%, 200tons and 215^{o}C respectively at the highest flexural strength value of 50.0933MPa. The predicted R^2 value of 99.97% and adjusted R^2 value of 99.99% are within 0.20 of each other indicating that the predicted response model and experimental data are in reasonable agreement (Mourabet et. al., 2013).

KEYWORDS: Numerical optimization, Flexural strength, Box – Behnken design, Experimental design, Regression statistics and Validation.

INTRODUCTION

Wood ash particles reinforced polypropylene (WARPP) composite has been investigated to determine its performance at optimal setting of parameters. The performance of WARPP is effected by many factors such as wood ash particle size, volume fraction, injection force and operating temperature of the injection moulding machine.

WARPP is a composite material that consist of polypropylene (PP) resin as the matrix material and wood ash particles as the filler material. Wood ash engineering application has been studied relatively by few researchers. Most of the applications had been to cement based work. Abdullahi (2006) in his paper titled "characteristics of wood ash/OPC concrete" reported that wood ash obtained from the combustion of wood can be related to fly ash since fly ash is obtained from coal, a fossilized wood. Okunade (2008) in his research article titled "the effect of wood ash and saw-dust admixture on the engineering properties of a burnt laterite – clay brick" stated that wood ash admixture in line with its pozzolanic nature was able to contribute in attaining denser products with higher compressive strength. Sanusi et. al., (2013) investigated the influence of wood ash as an additive on the mechanical properties of polymer matrix composite (fibre glass reinforced epoxy resin). The mechanical properties investigated include tensile strength, impact and hardness strengths. Result of the research revealed that addition of the wood ash into fibre glass reinforced epoxy resin composite improved the tensile strength and impact strength up to 2.3% and 0.8% of wood ash addition respectively. Hardness strength also increased progressively with the addition of wood ash. Naik et. al., (2001) researched on "wood ash: a new source of pozzolanic material". They

studied the physical, chemical and microstructural properties of wood ash in order to determine the potential applications for it. Goodman Mark Mendel (1998) conducted research on the effects of wood ash additive on the structural properties of lime plaster. The objective of the research was to determine the effects that wood ash imparted to lime plaster while focusing upon the performance criteria relevant to base coat application such as water retention, shrinkage, adhesion and permeability. However no application of wood ash was made in thermoplastic polymer resin.

In this study, a research on the application of wood ash particles as potential filler materials in polypropylene resin was conducted.

MATERIALS AND METHODS

1.1 Material Selection

The materials used in this research are thermoplastic polymer, polypropylene (PP) resin as a matrix material while wood ash particles were used as filler material. PP, a linear hydrocarbon polymer was obtained from a resin chemical commercial outfit named POKEZ chemicals at Onitsha while the wood ash (hardwood) was sourced locally. The wood ash was obtained from 10Kg mass of saw dust that was burnt and allowed to smouldered in an open space at ambient temperature for 12 hours. The characteristics (chemical compositions) of the wood ash obtained from X- ray Fluorescence analysis is presented in Table 1.

Compound oxides	*% composition*
* *Silicon Dioxide*, SiO_2	13.9
Titanium Oxide, TiO_2	0.76
* *Sulphur (vi) oxide*, SO_3	10.5
Iron Oxide, Fe_2O_3	4.31
* *Calcium Oxide*, CaO	45.2
* *Manganese Oxide*, MnO	1
* *Rubidium Oxide*, Rb_2O	0.055
Manganese Oxide, MnO	2.97
* *Strontium Oxide*, SrO	0.1
* *Indium (iii) Oxide*, In_2O_3	3.6
Copper (ii) Oxide, CuO	0.083
* *Potassium Oxide*, K_2O	15.1
Zinc Oxide, ZnO	2.24
* *Europium (iii) Oxide*, Eu_2O_3	0.07
* *Barium Oxide*, BaO	0.09

Table 1: Result of X – ray Fluorescence analysis of wood ash.

1.2 Chemical Modification of Wood Ash Particles Applied to Polypropylene.

Silane coupling agent was used as a chemical bonding agent in this work. The silane coupling agent was in liquid form and has the name 3 – aminopropyltrimethoxy silane. The chemical formula is $(CH_3O)_3 S_i CH_2 CH_2 CH_2 - NH_2$ and was supplied by Globemeth. The silane coupling agent was added without dilution to the filler materials by spraying method. The treated filler materials (wood ash particles) were added into the polypropylene resin in volume fractions of 5%, 35% and 60% before injection moulding to produce the samples. To investigate the bonding efficiency of the coupling agent, Fourier Transform Infrared Spectroscopy (FTIR) test was performed so as to analyze the molecular vibrations of the samples. The analyses were performed at Spring Board Chemical Research laboratory, Awka. Different spectra produced from the analyses represented the "fingerprints" of the samples with absorption peaks corresponding to the frequencies of vibrations of the bonds in the atom of the materials. The absorbance intensities of the bonds were identified and recorded. Absorbance intensity shows the influence of filler modification on light absorption of materials. The sample with the smallest value of absorbance intensity signify the most porous of all the samples. The spectra of three representative samples are presented and discussed in chapter 4.

1.3 Design of experiments.

Two experimental designs were applied in this work, namely Taguchi Robust Design (TRD) and Response Surface Methodology (RSM). Taguchi experimental design method consists of input variables that are divided into the following categories:

(i) Control factors: These are the design parameters of the product or process.

(ii) Noise (External) factors: These are factors whose values are difficult to control during normal production process (Unal & Dean, 1991).

Taguchi techniques consider only the main effects of a model, and these are the first order terms of the model. The limitations of Taguchi technique of not handling interaction effects were handled by the application of RSM. RSM is a second order function for approximating the response of factors with interaction effects. RSM model consists of first order and higher order terms. In the application of RSM method, two special experimental designs considered in fitting second order model to the response with minimum number of runs were:

(i) Central Composite Design (CCD) and

(ii) Box – Behnken Design.

A CCD with 3 design variables at 2 levels has 2^3 factorial points, 2 x 3 axial points and 1 central point (Hill and Hunter, 1966). Box – Behnken design is a three level factors design that are widely used in response surface methods to fit second order models to responses (Relia, 2013). The advantages of Box – Behnken design include:

(i) The fact that it is a spherical design and requires factors to be run at only three levels. That is all factorial and axial points are at the same distance from the center of the design.

(ii) There are no runs where all factors are at either +1 or -1 levels.

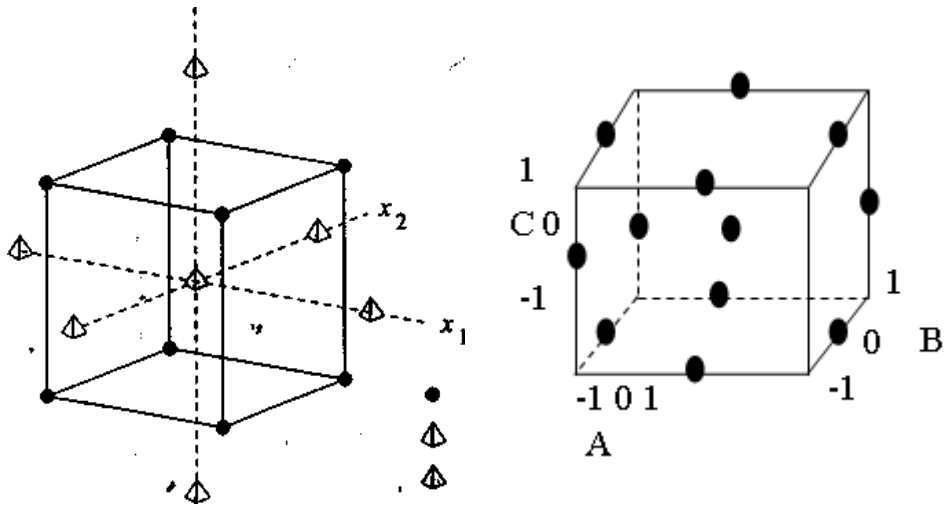

Figure 1(a): CCD for 3 design variables at 2 levels (b)Box - Behnken design for three factors at 3 levels.

1.4 Fitting a Second Order Model to the Design Data.

The limitation of TRD method of not handling interaction effects and RSM to handle noise effects was solved by extending the result of TRD with RSM.

The response function of a second order model is best characterized by multivariate power equation. The data obtained from Taguchi robust design was linearized on the assumption according to Chapra and Canale (2006) that the experimental result follow a power law model of the form:

$$Y = a_0 A^{a1} B^{a2} C^{a3} \ldots N^{an} \quad (1)$$

And that the response surface is optimized by a second order polynomial equation expressed as:

$$Y = \beta_O + \sum_{i=1}^{q} \beta_i X_i + \sum_{i=1}^{q} \beta_{ii} X_i^{\,2} + \sum_{i=1}^{q-1} \sum_{j=2}^{q} \beta_{ij} X_i X_j + \varepsilon \quad (2)$$

where Y is the predicted response used as a dependent variable,

q is the number of independent variables (factors),

X_i (i = 1, 2) is the input factors,

β_o is the constant coefficient, and

β_i, β_{ij} and β_{ii} are the coefficients of linear, interaction and quadratic terms respectively.

The coefficient parameters were estimated using regression as analysis tool for evaluating log data of input parameters presented in Table 2, and expressed as a power law model of the form of equation (2).

$$Y_{flex} = 7.041676689 * (A\text{^}0.0002) * (B\text{^}-0.0463) * (C\text{^}0.1053) * (D\text{^}0.2755) \quad (3)$$

Twenty – seven observed responses presented in Table 2 were obtained by evaluating equation (3) using the data values of the factors' levels of Box – Behnken design matrix.

Table 2: Experimental design matrix of Box – Behnken design for optimization of power function (equation) of flexural strength of PP composites.

Std order	*Run order*	*Blocks*	*Factor A: Particle size (mm)*	*Factor B: Volume fraction(%)*	*Factor C: Injection force(ton)*	*Factor D: Operating temp.)°C)*	*Response Y: Flexural strength (MPa)*
24	1	1	0.825	60	160	215	43.636
3	2	1	0.250	60	160	200	42.765
18	3	1	1.400	32.5	120	200	42.699
20	4	1	1.400	32.5	200	200	45.058
7	5	1	0.825	32.5	120	215	43.554
16	6	1	0.825	60	200	200	43.792
12	7	1	1.400	32.5	160	215	44.898
17	8	1	0.250	32.5	120	200	42.684
5	9	1	0.825	32.5	120	185	41.788
10	10	1	1.400	32.5	160	185	43.077
8	11	1	0.825	32.5	200	215	45.960
1	12	1	0.250	5	160	200	47.980
19	13	1	0.250	32.5	200	200	45.042
2	14	1	1.400	5	160	200	47.997
11	15	1	0.250	32.5	160	215	44.882
6	16	1	0.825	32.5	200	185	44.096
13	17	1	0.825	5	120	200	46.560
14	18	1	0.825	60	120	200	41.500
26	19	1	0.825	32.5	160	200	44.007
27	20	1	0.825	32.5	160	200	44.007
9	21	1	0.250	32.5	160	185	43.062
22	22	1	0.825	60	160	185	41.867
21	23	1	0.825	5	160	185	46.972
25	24	1	0.825	32.5	160	200	44.007
4	25	1	1.400	60	160	200	42.780
23	26	1	0.825	5	160	215	48.957
15	27	1	0.825	5	200	200	49.132

The response surface models were stated as equations (9) and (10) for coded and uncoded factors presented and discussed in chapter 4, section 4.2.

The test for statistical significance of the response model is presented in the analysis of variance (ANOVA) Table 3, and also as Table 4 in chapter 4, section 4.3, where it was discussed.

Table 3: Analysis of variance (ANOVA) for RSM optimization of WARPP for flexural strength.

Source	*DF*	*Seq SS*	*Adj. SS*	*Adj. MS*	*F – value*	*P – value*
Re *gression* mod*el*	14	121.916	121.916	8.7083	16865.82	0.000
Linear	4	108.581	108.581	27.1452	52573.70	0.000
A	1	0.001	0.001	0.0007	1.43	0.255
B	1	81.422	81.422	81.4219	157694.59	0.000
C	1	17.029	17.029	17.0289	32980.92	0.000
D	1	10.129	10.129	10.1292	19617.86	0.000
Square	4	13.301	13.301	3.3253	6440.37	0.000
A A*	1	0.401	0.000	0.0000	0.04	0.836
B B*	1	12.801	10.078	10.0784	19519.52	0.000
C C*	1	0.096	0.096	0.0964	186.75	0.000
D D*	1	0.003	0.003	0.0031	5.93	0.031
Interaction	6	0.034	0.034	0.0056	10.87	0.000
A B*	1	0.000	0.000	0.0000	0.00	0.966
A C*	1	0.000	0.000	0.0000	0.00	0.983
A D*	1	0.000	0.000	0.0000	0.00	0.983
B C*	1	0.020	0.020	0.0196	37.96	0.000
B D*	1	0.012	0.012	0.0117	22.59	0.000
C D*	1	0.002	0.002	0.0024	4.65	0.052
Re *sidual error*	12	0.006	0.006	0.0005		
Lack of fit	10	0.006	0.006	0.0006		
Pure error	2	0.000	0.000	0.0000		
Total	26	121.922				

Where A, B, C and D are the particle size, volume fraction, injection force and operating temperature respectively. The coefficients with the factors A, B, C and D represent the effects of the factors, while the coefficients with A^2, B^2, C^2, D^2 and those with A*B, A*C, A*D, B*C, B*D and C*D represent the quadratic effect and interaction between the two factors respectively.

The regression statistics, coefficient of determination (R^2) = 99.99%, R^2adj. = 99.99% and predicted R^2 = 99.97%. The coefficient of determination (R^2) indicates how much of the observed variability in the data was accounted for by the model. The adjusted coefficient of

determination (R^2adj) modifies R^2 by taking into account the number of predictors (terms) in the model. The R2adj. close to the R^2 value insured a satisfactory adjustment of the quadratic model to the experimental data. The predicted R^2 is a measure of how well the model predicted the response value. The R^2adj. and R^2pred. are within 0.20 of each other showing that they are in reasonable agreement (Mourabet et. al., 2013). The regression statistics can be checked using a numerical method for coefficient of determination (R^2), adjusted R^2 (R^2adj.) as expressed in equation (4) and (5) (Trinh and Kang, 2010).

$$R^2 = 1 - \frac{SS_{residual}}{SS_{\text{model}} + SS_{residual}} \quad (4) \qquad R^2{}_{adj.} = 1 - \frac{n-1}{n-p}\left(1 - R^2\right) \quad (5)$$

where SS is the sum of squares.

n is the number of experiments.

p is the number of predictors (terms) in the model, not counting the constant term.

3: Validation of the Model.

It is necessary to check the fitted model to ensure that it provides an adequate approximation to the real system. Unless the model shows an adequate fit, proceeding with the optimization of the fitted response surface is likely to give misleading result. The graphical optimization method i.e. optimization plot was used as a primary tool for optimization. The graphical technique was validated using numerical method. The crucial phase of numerical optimization is the assignment of optimization parameters. There are three optimization parameters namely maximum, minimum and target that define each desirability index, d_i. The desirability function d_i is defined differently based on the objective of the response according to Relia Wiki (2013) and is expressed as:

(i) If the response is to be maximized, d_i is defined as:

$$d_i = \begin{cases} 0 & Y_i < L \\ \left(\dfrac{Y_i}{T - L}\right)^1 & L \le Y_i \le T \\ 1 & Y_i > T \end{cases} \quad (6)$$

where T represents the target value of the i^{th} response (the highest value) and

L represents the acceptable lower limit value for the response.

(ii) If the response is to be minimized, di is defined as:

$$d_i = \begin{cases} \left(\dfrac{U - Y_i}{U - T} \right)^{1}_{0} & Y_i < T \\ & T \le Y_i \le U \\ & Y_i > U \end{cases} \quad (7)$$

Where U represents the acceptable upper limit of the response and T is the smallest value.

(iii)For a specific target response value, d_i is defined as:

$$d_i = \begin{cases} \left(\dfrac{\dfrac{Y_i - L}{T - L}}{\dfrac{U - Y_i}{U - T}} \right)^{0}_{0} & Y_i < L \\ & L \le Y_i \le T \\ & T \le Y_i \le U \\ & Y_i > U \end{cases} \quad (8)$$

By the evaluation of equation (6) for maximization as a desirability, using the maximum and minimum values of Flexural strength in Table 2 at desirability index $d_i = 1$, $Y_i > T$.

$$1 = \left(\frac{Y_i - 41.500}{49.132 - 41.500} \right)$$

Which gives $Y_i > 49.132$

From the optimization plot of Figure 5 presented and discussed in chapter 4 section 4.4, Y_i = 50.093MPa.

4 RESULTS AND DISCUSSIONS

4.1 Results of characterization of WARPP samples

The quality of WARPP samples used in this study was evaluated using microscopic method – Fourier transform infrared spectroscopy (FTIR) technique. Three different spectra were produced from three different samples. The spectra were represented by Figures 2, 3 and 4. Their vertical axes represent the absorption peaks while the horizontal axes are the wavenumbers.

Absorption

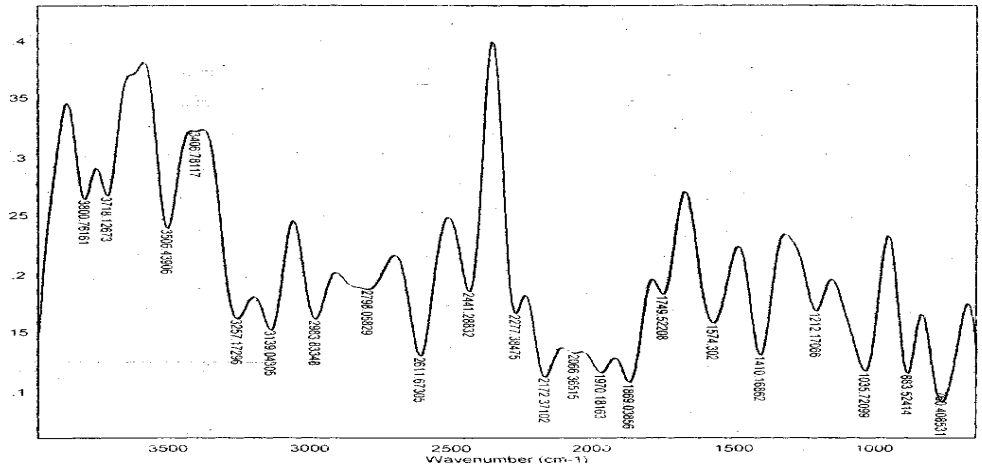

Figure 2: A plot of transmission against wave number of sample 1.

Sample 1: 0.25(5 % vol. fraction), from Figure 2 we have the following peaks.

3406.78- O-H stretch vibration (H bond)

2983.83 – C-H stretch vibration, (C-H) alkane group.

1749.52 – C=O stretch vibration

883.52 – C-H bend (deformation vibration).

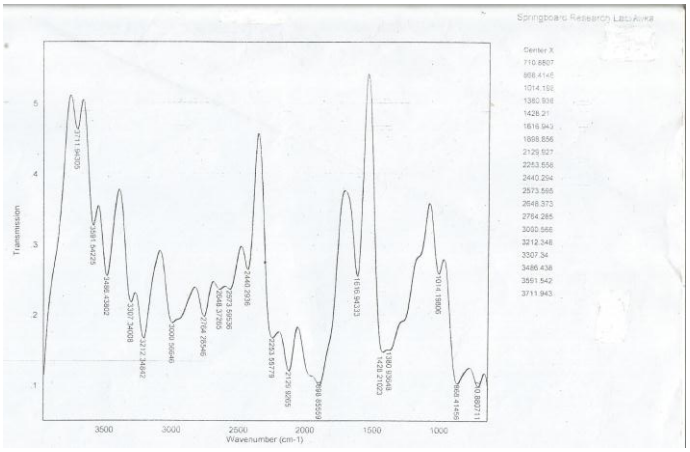

Figure 3: A plot of Transmission vs. Wave number of sample 1.40(35 % vol. fraction).

For sample 2: 1.40(35 % vol. fraction), from Figure 3 the absorption peaks are:

3486.43 – O-H stretch vibration

3000.56 – C-H stretch vibration

1616.94 – C = O stretch vibration

868.41 – C-H bend (deformation vibration)

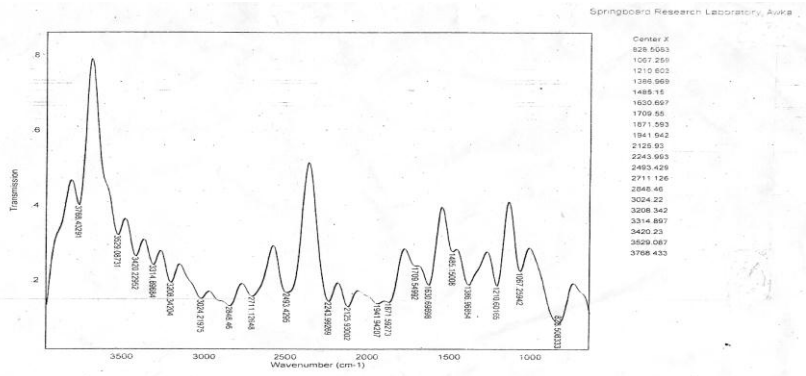

Figure 4: A plot of Transmission vs. wave number of sample 3.

For sample 3: 0.80(60 % volume fraction), from Figure 4 the absorption peaks are:

3420.22 – O – H stretch vibration.

3024.21 – C-H stretch vibration.

1709.54 – C=O stretch vibration

828.50 – C-H bend (deformation vibration).

The identifiable mode of vibration by the chemical bonds are stretch vibration and deformation vibration.

Discussion of the FTIR spectrum.

In Figure 2, the region of absorbance peaks is 3800.762cm^{-1} and 760.4085cm^{-1}, for the sample composition designated as 0.25(5% vol. fraction). Figures 3 and 4 had their absorbance peaks in the regions of 3711.943cm^{-1} and 710.881cm^{-1} for sample composition designated as 1.40(35% vol. fraction), and 3768.433cm^{-1} and 828.508cm^{-1} for the sample composition designated as 0.80(60% vol. fraction). The corresponding absorbance ranges are 3040.353cm^{-1}, 3001.062cm^{-1} and 2939.9247cm^{-1} respectively. The corresponding absorbance intensity range is 26.667 – 10.000 = 16.667%, 46 – 10 = 36%, and 40 – 10 = 30% respectively. Absorbance intensity indicates the influence of filler modification on light absorption. The lowest absorbance intensity value signifies that composite of the designated composition 0.25(5 % vol. fraction) may be more porous.

In Figure 2, where the intensity of absorption is 3406.78 cm^{-1} is showing strong hydrogen bonding with stretch vibration. The hydrogen bonding is due to de-methylation of the methoxyl group (-OCH_3) in silane coupling agent, which splited and CH_3 being replaced by hydrogen atom producing a new O-H group (Bykov, 2008). The 2983.83cm^{-1} band (peak) shows alkane (C-H) stretch vibration of the methoxyl group. The absorption band 883.52cm^{-1}

signifies deformation vibration (bending) of C-H bond. The absorption band 1,749.52 signifies the carboxyl, c = o stretch vibration.

Similarly, the absorption peak in Figure 3 is around 3486.43cm^{-1}. Also de-methylation of the methoxyl group in silane coupling agent occurred, and the methyl group was replaced by hydrogen atom. The absorption band 3000.56cm^{-1} is due to C-H stretch vibration of the methoxyl group. The absorption band 868.41cm^{-1} signifies deformation vibration of C-H bond.

In Figure 4, the peak is around 3420.22cm^{-1} and is due to the hydrogen bonding (O-H) stretch vibration. De-methylation also took place with the methoxyl group in silane coupling agent splited, creating condition for the production of hydrogen bond. The absorption band 868.41cm^{-1} is due to C-H deformation vibration.

4.2: Result of the evaluation and optimization of flexural strength of WARPP.

The response surface models are second order regression models that contain $15\{(n+1)(n+2)/2\}$ numbers of regression parameters, where n is the number of factors. The parameters include the coefficients for main effects A, B, C and D, coefficients for quadratic main effects A^2, B^2, C^2 and D^2 and the coefficients for two factor interaction effects A*B, A*C, A*D, B*C, B*D and C*D and a constant value.

For coded factor,

$$Y = 44.007 + 0.0078A - 2.6048B + 1.1913C + 0.9188D - 0.0021A\text{^}2 + 1.3747B\text{^}2 - 0.1345C\text{^}2 - 0.024D\text{^}2 - 0.0005A*B + 0.0003A*C + 0.0003A*D - 0.07B*C - 0.054B*D + 0.0245C*D. \quad (9)$$

For uncoded factor,

$$Y = 25.6945 + 0.0175116A - 0.176485B + 0.0505655C + 0.10154D - 0.0063012A\text{^}2 + 0.00181774B\text{^}2 - 8.40365E-05C\text{^}2 - 1.06481E-04D\text{^}2 - 3.16206E-05A*B + 1.08696E-05A*C - 2.89855E-05A*D - 6.36364E-05B*C - 1.30909E-04B*D + 4.08333E-05C*D \quad (10)$$

4.3: Test for statistical significance

Table 4: Analysis of variance (ANOVA) for RSM optimization of WARPP for flexural strength.

Source	*DF*	*Seq SS*	*Adj. SS*	*Adj. MS*	*F – value*	*P – value*
Re*gression* mod*el*	14	121.916	121.916	8.7083	16865.82	0.000
Linear	4	108.581	108.581	27.1452	52573.70	0.000
A	1	0.001	0.001	0.0007	1.43	0.255
B	1	81.422	81.422	81.4219	157694.59	0.000
C	1	17.029	17.029	17.0289	32980.92	0.000
D	1	10.129	10.129	10.1292	19617.86	0.000
Square	4	13.301	13.301	3.3253	6440.37	0.000
A A*	1	0.401	0.000	0.0000	0.04	0.836
B B*	1	12.801	10.078	10.0784	19519.52	0.000
C C*	1	0.096	0.096	0.0964	186.75	0.000
D D*	1	0.003	0.003	0.0031	5.93	0.031
Interaction	6	0.034	0.034	0.0056	10.87	0.000
A B*	1	0.000	0.000	0.0000	0.00	0.966
A C*	1	0.000	0.000	0.0000	0.00	0.983
A D*	1	0.000	0.000	0.0000	0.00	0.983
B C*	1	0.020	0.020	0.0196	37.96	0.000
B D*	1	0.012	0.012	0.0117	22.59	0.000
C D*	1	0.002	0.002	0.0024	4.65	0.052
Re*sidual error*	12	0.006	0.006	0.0005		
Lack of fit	10	0.006	0.006	0.0006		
Pure error	2	0.000	0.000	0.0000		
Total	26	121.922				

As can be seen from ANOVA Tables 4, the F - values obtained for the significant terms are greater than the F – value of 2.64 at 95% significance ($F_{0.95, 14, 12}$) of a standard F- distribution table. This confirmed the adequacy of the model fit. The significance of each term in the models was indicated by the p – values associated with the terms. A term is not significant if p – value is greater than 0.05. The value 0.05 indicates the significance level of observed effects. Significance level is the probability of the observed significant effect being due to pure error. That is, the risk of saying that a factor is significant when in fact it is not.

4.4 Optimization Plot.

Optimization plot is the graphical representation of the dependent and independent variables at their optimal settings. The optimal values of the factors were indicated in the plot. The optimization plot indicated a maximum predicted value of 50.0933MPa flexural strength with particle size of 1.40mm, volume fraction of 5%, injection force of 200tons and operating temperature of 215^{o}C. The result of the validation of model is in agreement with the result obtained from experiment and graphical model.

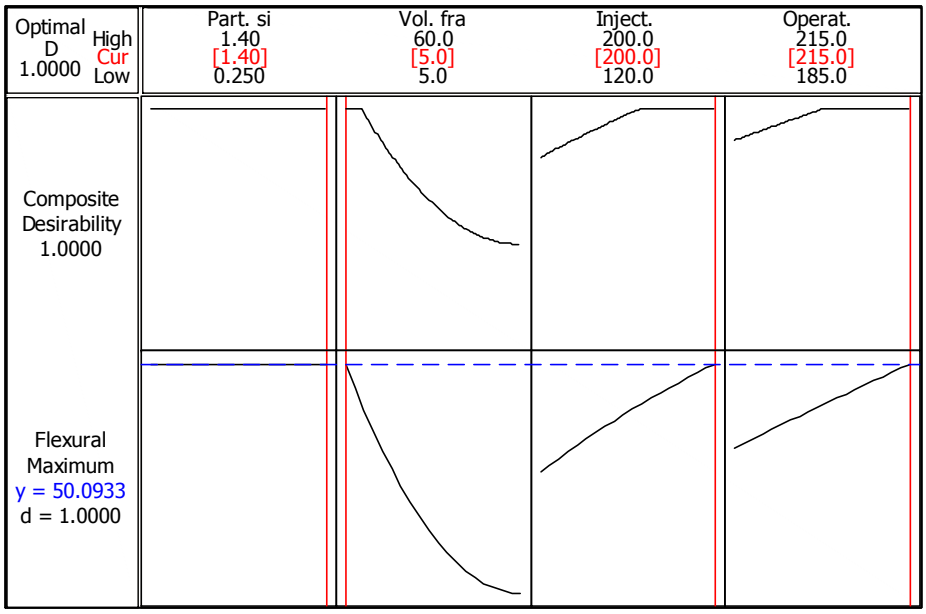

Figure 5: Optimization plot for flexural strength.

CONCLUSIONS

This work has demonstrated the application of Numerical optimization in validating the optimized performance characteristics of flexural strength of WARPP. From the study carried out, the following conclusions were drawn:

1. The result of statistical analysis (ANOVA) shows that the control and interaction factors B, C, D and B*B, C*C, B*C and B*D have significant effects on the flexural strength of WARPP.
2. The flexural strength of WARPP is in the range of 46.65MPa – 50.09MPa.
3. The response model of WARPP is representable with nonlinear power law and second order polynomial equation.
4. The optimal value of flexural strength of WARPP was obtained with the particle size of 1.40mm, volume fraction of 5%, injection force of 200tons and operating temperature of 215^{o}C.
5. The results of the optimization plot were obtained at a condition (desirability = 1) that satisfied each of the parameters without compromising on any of them (i.e. they are equally weighted). This demonstrated that to obtain a maximum amount of information in a short period of time, with the least number of experiments, RSM and optimization plot can be successfully applied for modeling and optimizing the flexural strength of WARPP.
6. The flexural strength of WARPP obtained from the validation of the model is in the range of that estimated using the model. This implied that the numerical optimization approach

was appropriate for validating the optimized performance characteristics of flexural strength of WARPP.

REFERENCES

1. Abdullahi M. Characteristics of Wood Ash/OPC Concrete. Leonardo Electronic Journal of Practices and Technologies, 2006; (8): 9-16.
2. Chapra S. C., and Canale R. P. Numerical Methods for Engineers. 5th Edition, McGraw-Hill, New York, 2006; 460 – 462 and 623 – 625.
3. Goodman M. M. The effects of wood ash additive on the structural properties of line, 1998. plaster. [Online]. Available: http://archive.org/stream/effects of woodashoogood/effectsofwoodash.
4. Hill W. J and Hunter W. G. A review of response surface methodology: A literature survey, 1966. Technometrics, 571- 591. Mead, R. and D. J. Pike… [Online]. Available: www.stat.rudgers.edu/home/buyske/591/Lect06.pdf
5. Mourabet M., El Rhilassi A., El Boujaady H., Bennani-Ziatni M., Taitai A. Use of Response Surface Methodology for Optimization of Fluoride adsorption in an aqueous Solution by Brushite. Arabian Journal of Chemistry, 2013; 12: 028.
6. Naik Tarun R., Kraus Rudolph, and Kumar R. Wood Ash: A new source of Pozzolanic material. Report No. CBU Centre for by-product utilization. University of Wisconsin, 2001.
7. Okunade E. A. The Effect of Wood Ash and Sawdust Admixtures on the Engineering Properties of a Burnt Latrite-Clay. Journal of Applied Sciences, 2008; 8: 1042-1048.
8. Radharamanan R. and Ansui A. P. Quality Improvement of a Production Process using Taguchi Methods. Proceedings of Institute of Industrial Engineers' Annual Conference, Dallas, Texas, 2001.
9. Relia Wiki: Response Surface Methods for Optimization. [Online]. http://reliawiki-org/index.php/Response_Surface_methods_for_opti.. (Accessed Sept. 19), 2013.
10. Sanusi O. M., Oyinlola A. K., Akindapo J. O. Influence of Wood Ash on the Mechanical properties of Polymer Matrix Composite Developed from Fibre glass and Epoxy resin. International Journal of Engineering Research and Technology (IJERT). ISSN 2278 – 0181, 2013; 2(12).
11. Suresh R. K. Multi Objective Optimization during Turning of AISI 8620 Alloy Steel using Desirability Function Analysis. International Journal of Engineering Science & Research Technology, 2014; 3(10).

12. Trinh T. K. and Kang L. S. Application of Response Surface Method as an Experimental Design to Optimize Coagulation Tests. Journal of Environmental Engineering Research, 2010; 15(2): 63 – 70.
13. Unal R. & Dean B. Taguchi Approach to Design Optimization for Quality and Cost: An Overview. Presented at the Annual Conference of the International Society of Parametric Analysis, 1991.